Scanning Microscopy Vol. 12, No. 1, 1998 (Pages 113-118) 0891-7035/98$5.00+.25
Scanning Microscopy International, Chicago (AMF O'Hare), IL 60666 USA

CORRELATION BETWEEN SCANNING TUNNELING MICROSCOPY (STM)-INDUCED PHOTON MAP AND THE STM TOPOGRAPHY OF NANOMETER-SIZE METAL PARTICLES

R. Nishitani[1]*, T. Umeno[1], A. Kasuya[2] and Y. Nishina[2]

[1]Dept. Computer Science and Electronics, Kyushu Institute of Technology, Iizuka, Fukuoka 820, Japan
[2]Institute for Materials Research, Tohoku University, Katahira, Sendai 980-77, Japan

(Received for publication June 12, 1996 and in revised form October 7, 1996)

Abstract

We have measured the maps of integrated photon intensity and isochromat photon intensity induced by scanning tunneling microscopy (STM) of noble metal particles on the graphite surface. We have studied the correlation between the contrast of the photon maps with the STM topography. The integrated intensity of the photon map is closely correlated with the height of the topography image. The isochromat photon map changes depending on the wave length of the light collected. This change is explained by the effect of the variation in the tip curvature radius on the spectra of local plasmon. The emission intensity does not change with the size of the Au particle in the range from 3 to 20 nm on the substrate. The tip geometry has an effect on the emission intensity as well as the spectra.

Key Words: Scanning tunneling microscopy (STM), tunneling induced luminescence, local analysis, local plasmon, scanning probe spectroscopy, scanning probe microscopy, metal particles, graphite, gold, silver.

*Address for correspondence:
Ryusuke Nishitani,
Department of Computer Science and Electronics,
Kyushu Institute of Technology,
Iizuka, Fukuoka 820,
Japan

Telephone number: (81) 948 29 7670
FAX number: (81) 948 29 7651
E.mail: nisitani@cse.kyutech.ac.jp

Introduction

The photon emission from metal surfaces induced by electron tunneling in scanning tunneling microscopy (STM) has attracted considerable interest for the surface analysis at nanometer scale because the intensity map reflects various surface properties in the high resolution of the STM [1, 2, 3, 4, 5, 6, 7, 9, 10, 12, 13, 14]. Some researchers have succeeded in obtaining the STM induced photon maps with a nanometer scale or atomic scale resolutions in ultra high vacuum (UHV) [2, 7], as well as in air [12, 14]. However, the interpretation of the contrast in the photon maps is not straightforward because the photon emission is caused through various processes in STM junction.

The photon emission from STM junction is interpreted as radiation from the local plasmon which is excited by inelastic electron-tunneling near the local region between the STM tip and sample metals [1, 5, 6, 10]. The nature of the plasmon is determined with the boundary conditions of potentials of the STM tip and the metal surface [5, 10, 13]. Thus, the spectra from the local plasmon should be closely related to the geometric structure of the STM tip and the metals being sampled. In addition, the probability of inelastic tunneling for the plasmon excitation depends on the local density of states.

In order to interpret the contrast of the photon map, we need to know the relation between geometric structures of the STM tip apex and the sample surface and the photon spectra and the photon intensity. Berndt *et al*. [1] and Ito *et al*. [4] have measured spectra of STM induced light for metals. The spectra, however, have been recorded separately from the recording of the STM image. The measurements of spectral resolved photon map has not been made so far.

In order to study this geometric effect on the STM induced photon spectra as well as the local electronic structure of various materials at a nanometer scale, we need to obtain the spectral mapping of the STM induced light with the simultaneous measurement of STM images.

In this paper, we report the correlation between STM-induced photon map and the STM topography of nanometer-size metal particles. We have measured the spectral resolved map of STM induced light together with the simultaneous measurements of STM topography images. The isochromat

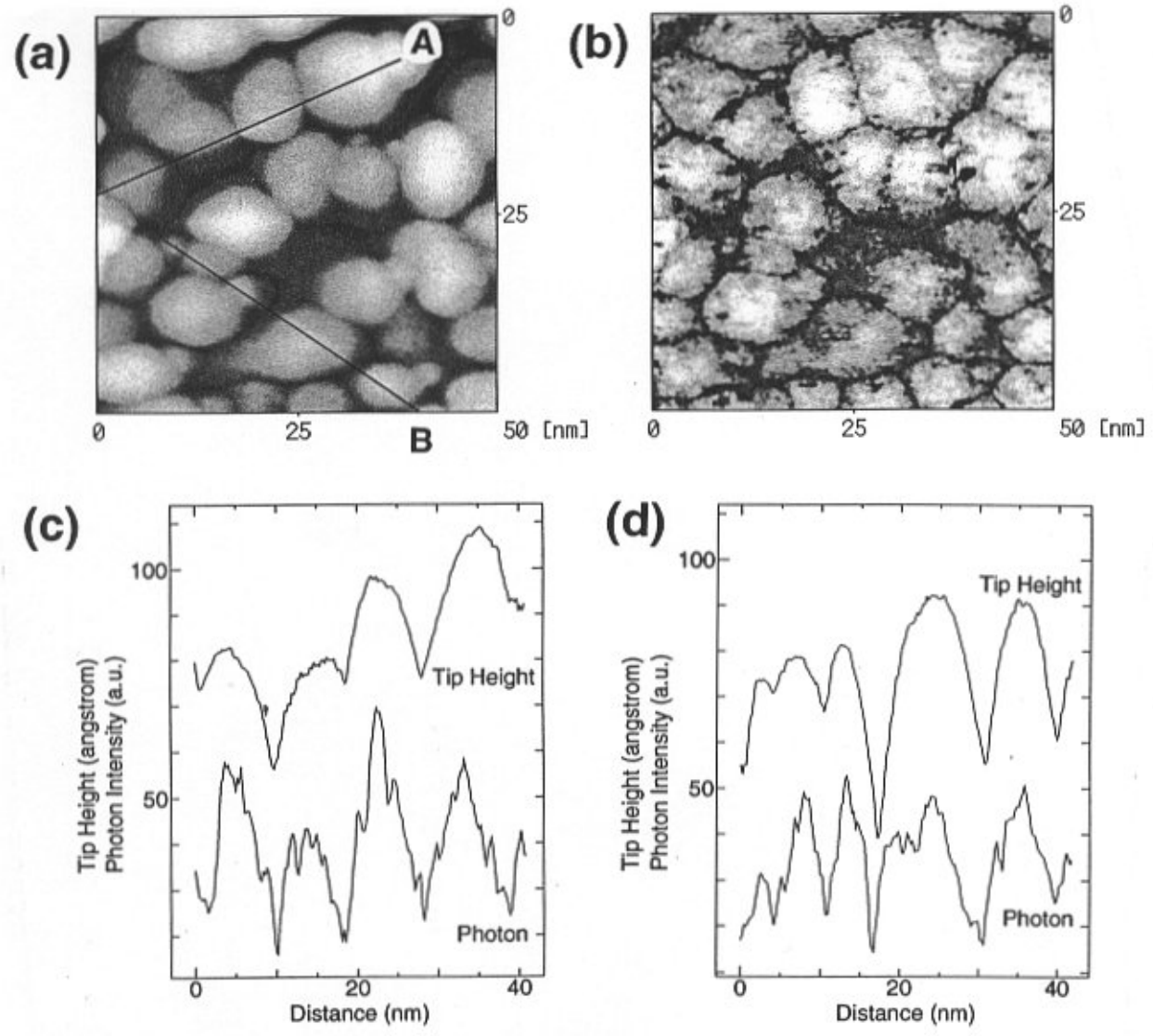

Figure 1. (**a**) STM image of gold particles (scan area 50 nm x 50 nm, current 3 nA, sample bias +2 V). (**b**) Integrated photon intensity map. (**c**) The height in STM and photon intensity of the photon map along a line A in Figure 1a. (**d**) The height in STM and photon intensity of the photon map along a line B in Figure 1a.

photon maps show that the spectra varies with the tip position. The results indicate the effect of the geometric asymmetry of the STM tip on the spectra.

Experiment

We have carried out a photon mapping measurement by using an in house-made UHV-STM combined with the photon detection system. For the STM control and the photon data acquisition, a digital computer system with microcomputers and a digital feed back controller is employed instead of an analog control system because variable and complex data-acquisition is easily realized by changing the software without a significant change of the hardware [8]. We have used a digital signal processor (DSP; TMS320C30, Texas Instruments, Dallas, TX) for the digital feed back control of STM.

Photons emitted from the tip-sample junction are collected using an ellipsoidal mirror. The focused photon is guided to a photomultiplier (Hamamatsu, R943-02) through

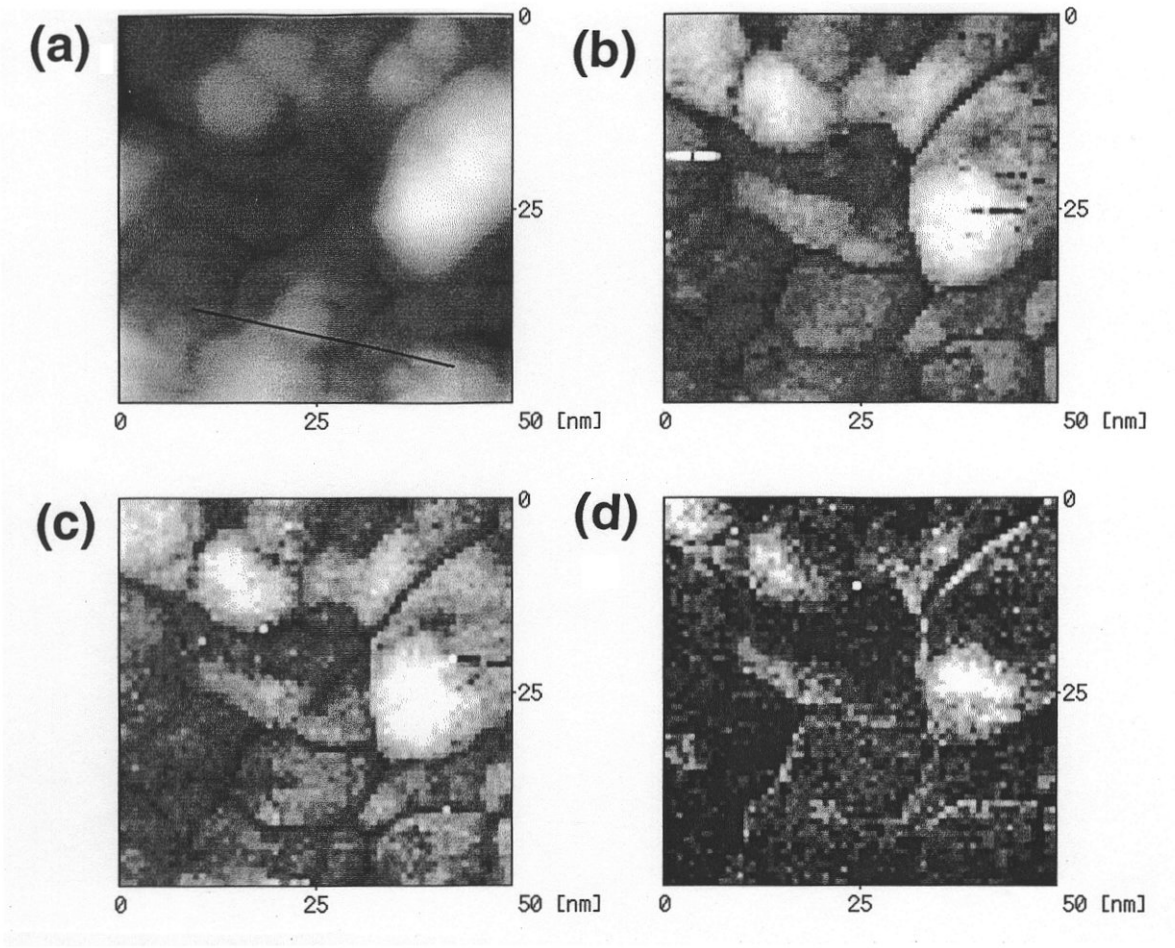

Figure 2. (**a**) STM image of silver particles (current 10 nA, sample bias +2 V, scan area 50 nm x 50 nm). (**b**) Integrated photon intensity map without an optical filter. (**c**) Isochromat photon map with a filter of 700 nm. (**d**) Isochromat photon map with a filter of 650 nm.

an optical fiber.

An isochromat photon map is measured by using optical band pass filters with the center of the wavelength of 700 nm and 650 nm and band widths of 80 nm and 30 nm, respectively. A photon map image with 64 x 64 or 128 x 128 pixels is obtained simultaneously with the STM topography image with 256 x 256 pixels. The photon count is integrated for 0.1 or 0.05 seconds at 64 x 64 points or 128 x 128 points in the scan region, respectively. The time for obtaining an photon image is limited by the time for photon counting and is about 7 minutes. The measurements was made at the sample bias of +2.0 V. The photon intensity ranges from 1000 to 20000 cps at the tunneling current of 10 nA depending on the condition of the tip and the surface. Photon maps observed have revealed a spatial resolution of less than 1 nm.

To study the correlation between photon maps and STM topography, a number of photon maps and topography images are measured for Au and Ag particles on the graphite surfaces. Gold or silver metal films are deposited on the graphite surface by thermal evaporation in a high vacuum of about 1 x 10^{-7} Torr, and transferred to an UHV chamber for STM measurements without exposing to air. The graphite surface was prepared by cleavage in air before introducing into the chamber. The tunneling tips used in the experiments were made by electrochemically etching tungsten wire.

Results and Discussion

We have focused our attention on the following: (**1**) the correlation between the contrast of the integrated photon maps with the STM topography; (**2**) the relation between the integrated photon intensity with the particle size; and (**3**) emission intensity and the tip radius.

Figure 1 shows a topography image of Au grains (Fig.

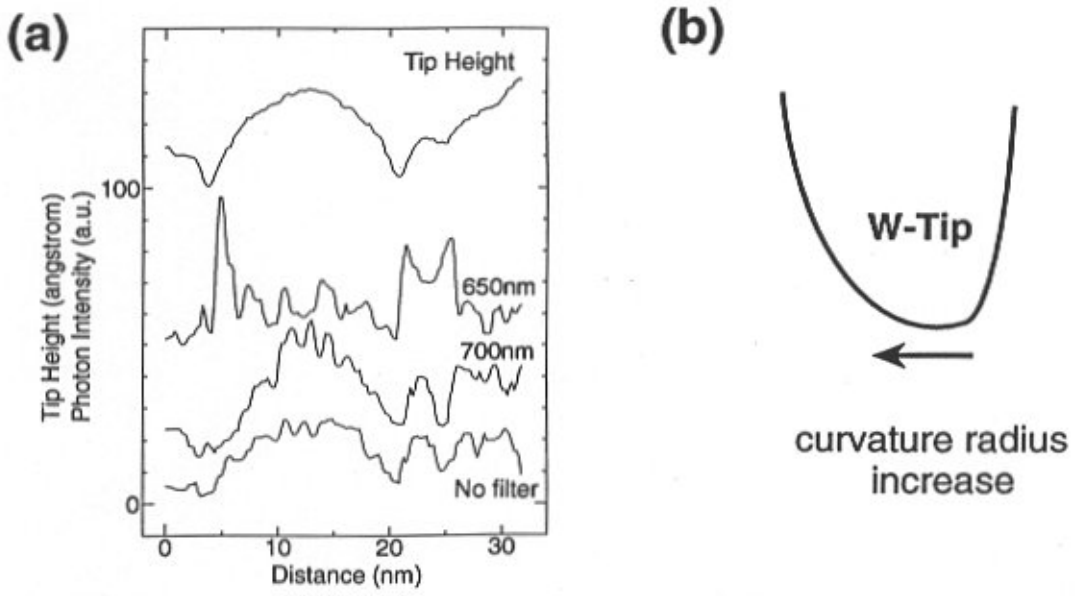

Figure 3. (**a**) Comparison of cross sections of topography and the photon maps. (**b**) A sketch of the proposed tip shape.

1a) and a simultaneously recorded photon map (Fig. 1b) of a corresponding scan area to the STM image. Photon intensity is recorded at 128 x 128 points out of 256 x 256 points of the STM image in the scan area of 50 nm x 50 nm. The photon map shows similar contrasting particles to those on the corresponding topography. Figure 1c compares the cross section of STM topography with the photon intensity map on a line A across the particles. The photon intensity is linearly correlated with the height of the grains in the STM image. The reason for the close correlation is not clear, but various factors should be considered. When the tip is located near the top of the grains, the tunneling current from the apex of the tip contributes to the excitation of plasmon which finally results in light emission. On the other hand, when the tip is located at the topographic valley between the grains, the tunneling location moves away from the apex of the tip. Therefore, the possible origin of the contrast of the photon map may be related to the tunneling-location as follows: (1) the change in the local density of states influences the probability of plasmon excitation; (2) the change in the local work function of tip and sample modifies the local barrier height; and (3) the most probable origin is related with the direction of STM induced dipole which is produced at the nearest point between STM tip and a particle, and depends on the tip location on the particle. The component of the dipole normal to the surface may be linearly dependent on the tip height because it varies as cos(θ), here θ is the angle between the surface normal and the dipole moment. Therefore, the photon intensity from this dipole may be closely correlated with the tip height. In this case, we should calculate the θ dependence of the power of the unpolarized light radiated from this dipole under consideration of the effect of the substrate.

Next, we discuss the effect of grain size on the photon intensity. The film shown in Figure 1 contains various sizes of grains. The STM image in Figure 1a indicates sizes ranging from 3 to 20 nm. The photon map also reveals corresponding sizes. The height in STM and the photon intensity of the photon map are plotted in Figure 1d along line B as shown in Figure 1a. The light intensity has no correlation with grain size, but is nearly constant although the grain sizes change from 3 to 20 nm. This observation is not consistent with Persson and Baratoff [10] predicting that the light emission changes with sphere size.

Figures 2a through 2d show a topography image of Ag grains (Fig. 2a) and simultaneously recorded photon maps (Figs. 2b, 2c, and 2d) of the corresponding area with and without an optical band pass filter. Figure 2b shows an integrated photon map without a filter, Figures 2c and 2d an isochromat photon map with a filter of 700 nm and 650 nm, respectively. The image of Figure 2a is recorded simultaneously with the photon map of Figure 2b, but the isochromat photon maps of Figures 2c and 2d are measured in separate scans of the same area of Figure 2a later, hence a few nanometer drift of the images appear between photon maps.

The integrated photon map (Fig. 2b) and an isochromat photon map of 700 nm (Fig. 2c), show a close correlation with

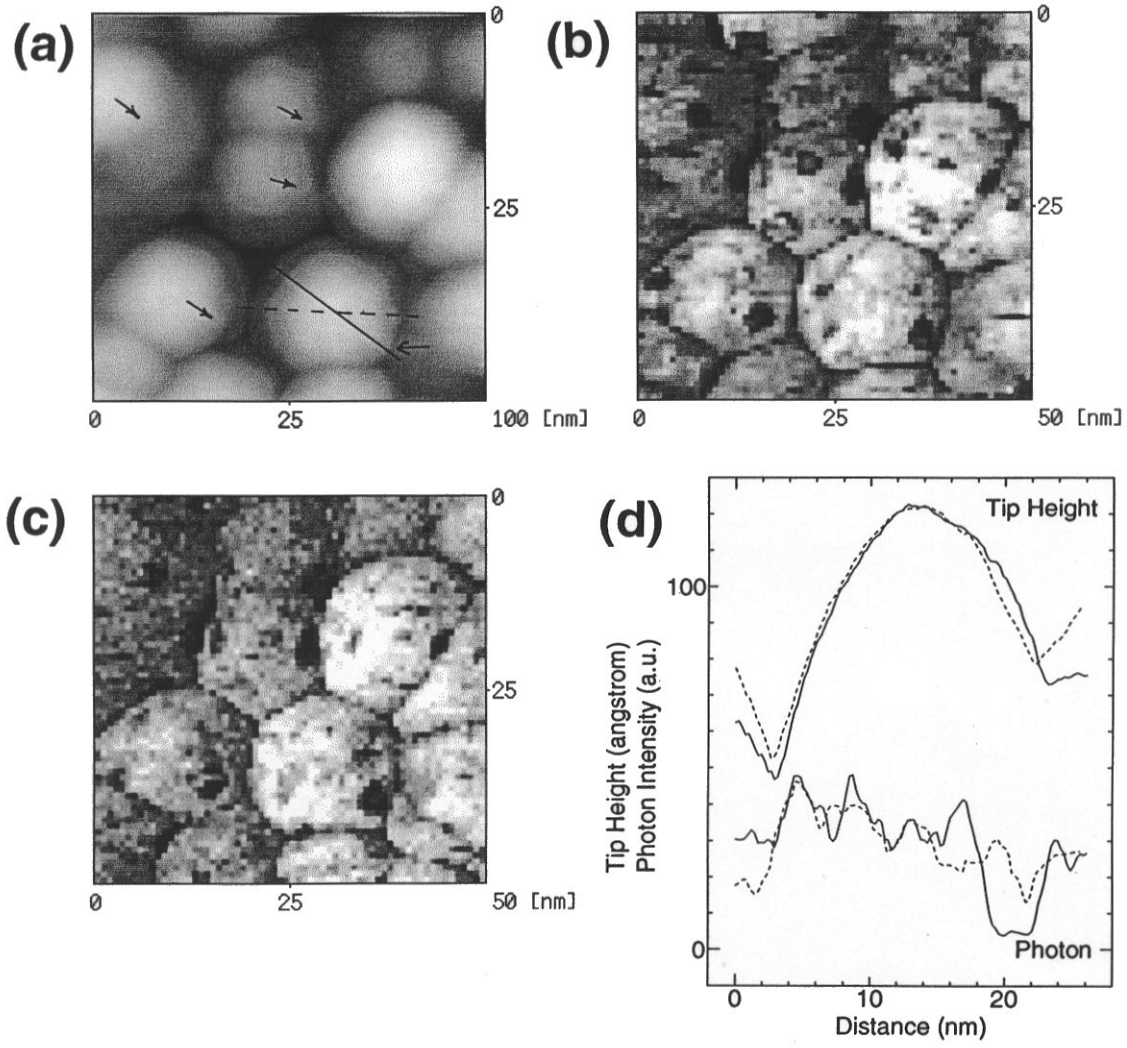

Figure 4. (**a**) STM image of gold particles (current 20 nA, sample bias +2 V, scan area 50 nm x 50 nm). Arrows indicate protrusions on the particles. (**b**) Integrated photon intensity map without an optical filter. (**c**) Isochromat photon map with a filter of 700 nm. (**d**) Cross-sectional profiles across the protrusion (solid line) compared with that along the dashed line which does not cross the protrusion.

---

the topography image (Fig. 2a). In the 650 nm photon map (Fig. 2d), on the other hand, we can see a different contrast from those in Figures 2a, 2b and 2c. In the isochromat map of 650 nm, the photon emission is enhanced near the left edge of the grains. In Figure 3a, the cross sections of the topography and the photon maps along a line in Figure 2a are shown. The result suggests that the location of the tip influences the spectra. As a origin of this contrast, two possibilities are considered. One is an excitation of a different mode plasmon near the valley between grains. Alternatively, an effect of the tip asymmetry on the plasmon excitation is possible. The former possibility, however, may be excluded because, in that case, the photon emission should be enhanced on both sides of the grains. If the tip had a symmetric shape, the asymmetry observed should not result for spherical grains. Thus, this phenomenon should be related to an asymmetry of the apex of the STM tip. Therefore, we assume an asymmetric shape as schematically shown in Figure 3b. The tip in the figure has a larger curvature radius on the left side of the tip than the right side. The observed change in the contrast of the isochoromat photon map in Figure 2d is explained by considering that the smaller tip radius enhances the photon intensity with a shorter wave length. When the tip is located on the left side of the grains, a part of the tip with a smaller tip

radius contributes to electron tunneling for the plasmon excitation, resulting in the increase in the intensity of shorter wave length light as observed in the contrast of photon maps in Figure 2d. This interpretation of tip radius dependence on the spectra is consistent with the theoretical prediction of the spectra of the local plasmon [11].

Figures 4a, 4b and 4c show a topography image of Au grains (Fig. 4a) and corresponding photon maps (Figs. 4b and 4c) with and without an optical band pass filter of 700 nm. In the photon map, dark regions of 10 nm size in diameter are seen at the right lower sides of the grains. In the STM topography image, small protrusions on the spheres are observed corresponding to dark regions in the photon map as indicated by arrows in Figure 4a. The cross sectional profile across the protrusion (solid line) is compared in Figure 4d with the cross section along the line which does not cross the protrusion (dashed line). This protrusion should be caused by a tip asymmetry like a metallic protrusion on the tip. The protrusion is not due to a non-metallic impurity because the STM image should show a hole if the non-metallic protrusion exist on the tip. From the cross section in Figure 4d, the height of the protrusion is about 1 nm at least, and the width is less than 10 nm. The curvature radius of the protrusion on the tip is estimated to be about 5 nm. The dark regions are observed in both photon maps regardless of the use of the optical filter, Figures 4b and 4c. Therefore, the dark region is not related to a drastic change in the spectrum of emitted light, but mainly to the decrease in the photon emission instead of the spectral change of the light emitted there. Therefore, the dark region in the photon map is interpreted in terms of the change in the emission intensity with the tip radius.

Conclusion

Maps of isochromat and integrated photon intensity of light induced by STM are obtained simultaneously with topography images. Comparison between the photon map and the STM topography shows the following facts. The integrated photon map is linearly correlated with the height of the STM image. The emission intensity does not depend on the particle size. This result is inconsistent with the theoretical prediction by Persson and Baratoff [10]. The contrast of the isochromat photon map is influenced by the tip geometry which induces the change in the emission spectra. The emission intensity seems to depend on the tip radius.

Acknowledgments

This work is supported in part by a Grant-in-Aid from the Ministry of Education, Science and Culture, and the Research Foundation For Materials Science.

References

[1] Berndt R, Gimzewski JK (1991) Inelastic tunneling excitation of tip-induced plasmon modes on noble-metal surfaces. Phys Rev Lett **67**: 3796-3799.

[2] Berndt R, Gimzewski (1993) Photon emission in scanning tunneling. J Phys Rev **B48**: 4746-4754.

[3] Gimzewski JK, Reihl B, Coombs JH, Schlittler, RR (1988) Photon emission with the scanning tunneling microscope. Z Phys B **72**: 497-501.

[4] Ito K, Ohyama S, Uehara Y, Ushioda S (1995) STM light emission spectroscopy of surface microstructures on granular Au films. Surf. Sci. **324**: 282-288.

[5] Johansson P, Monreal R, Apell P (1990) Theory for light emission from a scanning tunneling microscope. Phys Rev B **42**: 9210-9213.

[6] Johansson P, Monreal R (1991) Theory for photon emission from a scanning tunneling microscope. Z Phys B: Condensed Matter **84**: 269-275.

[7] McKinnon AW, Welland ME, Wong TMH (1993) Photon-emission scanning tunneling microscopy of silver films in ultrahigh vacuum: A spectroscopic method. Phys Rev B **48**: 15250-15255.

[8] Nishitani R, Suga K, Miyasato T (1993) Scanning tunneling microscope controlled by DSP. In: Abstract of 40th International Field Emission Symposium. International Field Emission Society. Nagoya, Japan. p. 144 (abstract).

[9] Nishitani R, Suga K, Umeno T, Kasuya A, Nishina Y (1996) Measurements of photon intensity map for metal particles by scanning tunneling microscopy. Material Science and Engineering, A MSA217/218: 99-102.

[10] Persson BNJ, Baratoff A (1992) Theory of photon emission in electron tunneling to metallic particles. Phys Rev Lett **68**: 3224-3227.

[11] Rendell RW, Scalapino DJ (1981) Surface plasmons confined by microstructures on tunnel junctions. Phys Rev B **24**: 3276-3294.

[12] Sivel V, Coratger R, Ajustron F, Beauvillain J (1992) Photon emission stimulated by scanning tunneling microscopy in air. Phys Rev B **45**: 8634-8637.

[13] Uehara Y, Kimura Y, Ushioda S, Takeuchi K (1992) Theory of visible light emission from scanning tunneling microscope. Jpn J Appl Phys **31**: 2465-2469.

[14] Venkateswaran N, Sattler K, Xhie J, Ge M (1992) Photon emission from nano-granular gold excited by electron tunneling. Surf. Sci. **274**: 199-204.

Editor's Note: All reviewers' comments were answered by text changes, hence there is no **Discussion with Reviewers**.